



ALMA MATER STUDIORUM · UNIVERSITÀ DI BOLOGNA

---

---

Physics and Astronomy Department  
PhD Thesis in Applied Physics

## Implementation and optimization of algorithms in Biomedical Big Data Analytics

**Supervisor:**

**Prof. Daniel Remondini**

**Correlator:**

**Prof. Gastone Castellani**

**Prof. Armando Bazzani**

**Presented by:**

**Nico Curti**

**Session 2019/2020**



# Chapter 1

## Feature Selection - DNetPRO algorithm

After the end of the Human Genome Project (HGP, 2003) [23] there were growing interest on biological data and their analysis. At the same time, the availability of this type of data increased exponentially with the technological improvement of data extractors (High-Throughput technologies) [26] and the lower production costs. Lower costs and efficiency in time extraction are the main factors that allow us to go into the new scientific era of Big Data. Biological Big Data works with very large and complex datasets which are typically impossible to store, handle and analyze using standard computer and techniques [19]. Just think that we need around 140 Gb for the storage of the DNA of a single person and an Array Express, a compendium of public gene expression data, contains more than 1.3 million of genomes which have been collected in more than 45000 experiments [13]. Since the number of available data is getting greater, we need to design several storage databases to organize, classify and moreover to extract information from them. The Bioinformatics European Institute (EBI) at Hinxton (UK), which is part of the European Laboratory of Biological Molecular and one of the biggest repositories of biological data, stores 20 petabytes of genomic data and proteomics back-ups. The amount of the genomics data is only 2 petabytes, and it doubles every year: it is not worth to remark that these quantities represent about a tenth of data stored by CERN of Ginevra [22]. In contrary, the ability of processing data and the computational techniques of analysis do not grow the same way. Therefore the gap between the great growth of the number of available data and our ability to work with them is getting bigger.

From a computational point of view, the Bioinformatics new-science is looking for new methods to analyze these large amount of data. The common Machine Learning methods, i.e computational algorithms able to identify significant patterns into large quantities of data, needs to be optimized and modified to increase their computational and statistical performances. To improve the computational times, we need to extend existing methods and algorithms and to develop new dimensionality reduction techniques. In Machine Learning, in fact, as the dimensionality of the data increases, the amount of data required to perform a reliable analysis grows exponentially<sup>1</sup>. The dimensionality reduction techniques are the methods able to identify the more significant variables of a given problem or a combination of them, where “significant” means that this smaller number of variables (or features) preserves the information about the problem as much as possible. So this huge amount of high-dimensional omics data (e.g. transcriptomics through microarray or NGS, epigenomics, SNP profiling, proteomics and metabolomics, but also metagenomics of gut microbiota) poses enormous challenges on how to extract useful information from them.

---

<sup>1</sup> High dimensional data tends to become very sparse and as consequence it is hard to perform robust statistical evaluation on it. This phenomena is commonly called “curse of dimensionality” [4].

One of the prominent problems is to extract low-dimensional sets of variables – signatures – for classification and diagnostic purposes, or to better stratify patients for personalized intervention strategies based on their molecular profile [28, 7, 17, 2].

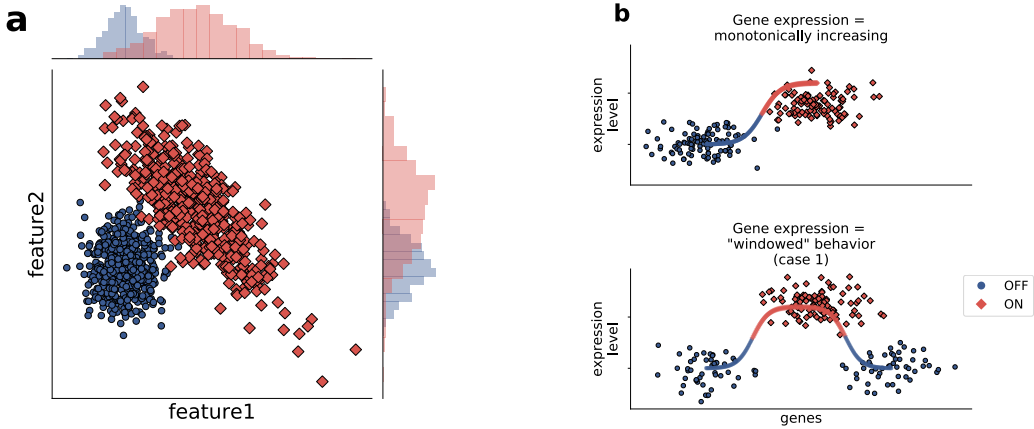


Figure 1.1: (a) An example in which single-parameter classification fails in predicting higher-dimension classification performance. Both parameters (*feature1* and *feature2*) badly classify in 1-D, but they have a very good performance in 2D. Moreover, classification can be easily interpreted in terms of relative higher/lower expression of both probes. (b) Activity of a biological feature (e.g. a gene) as a function of its expression level: top) monotonically increasing, often also discretized to an on/off state; center, bottom) “windowed” behavior, in which there are two or more activity states that do not depend monotonically on expression level. X axis: expression level, Y axis, biological state (arbitrary scales).

Many approaches are used for these classification purposes [14], such as Elastic Net [16], Support Vector Machine, K-nearest Neighbor, Neural networks and Random Forest [25]. Some methods select signature variables by means of single-variable scoring methods [12, 15] (e.g. Student’s t test for a two-class comparison), while others search for projections in variable space and then perform a dimensionality reduction by thresholding the projection weights, but these approaches could fail even in simple two-dimensional situations (Fig. 1.1).

Methods that select variables for multi-dimensional signatures based on single-variable performance can have limits in predicting higher-dimensional signature performance. As shown in Fig. 1.1(a), both variables taken singularly perform poorly, but their performance becomes optimal in a 2-dimensional combination, in terms of linear separation of the two classes.

It is known that complex separation surfaces characterize classification tasks associated to image and speech recognition, for which Deep Networks are used successfully in recent times, but in many cases biological data, such as gene or protein expression, are more likely characterized by an up/down-regulation behavior (as shown in Fig. 1.1(b) top), while more complex behaviors (e.g. a “windowed” optimal range of activity, Fig. 1.1(b) bottom) are much less likely. Thus, discriminant-based methods (and logistic regression methods alike) can very likely provide good classification performances in these cases (as demonstrated by our results with DNetPRO) if applied in at least two-dimensional spaces. Moreover, the “linearity” of these methods (that generate very simple class separation surfaces, i.e. linear or quadratic) ensures that a “buildup” of a signature based on lower-dimensional signatures is feasible.

These considerations are relevant in particular for microarray data, where we face on a small number of samples compared to a huge amount of variables (gene probes). This kind of problem, often called “large  $N$ , small  $S$ ” problem (where  $N$  is the number of features,

i.e variables, and  $S$  is the number of samples), tend to be prone to overfitting<sup>2</sup> and they are classified to ill-posed. The difficulty on the feature extraction can also increase due to noisy variables that can drastically affect the machine learning algorithms. Often, it is difficult to discriminate between noise and significant variables, even more as the number of variables rises.

In this thesis I propose a new method of features selection - DNetPRO, *Discriminant Analysis with Network PROcessing* - developed to outperform the mentioned above problems. The method is particularly designed to gene-expression data analysis and it was tested against the most common feature selection techniques. The method was already applied on gene-expression datasets but my work focused on the benchmark of it and on its optimization for Big Data applications. The pipeline algorithm is composed by many different steps and only a part of it was designed to biological application: this allow me to apply (part of) the same techniques also in different kind of problems with good results (see next sections).

## 1.1 DNetPRO algorithm

The DNetPRO algorithm generates multivariate signatures starting from all couples of variables tested with Discriminant Analysis. For this reason, it can be classified as a combinatorial method and the computational time for variable space exploration is proportional to the square of the number of available variables (ranging from  $10^3$  to  $10^5$  in a typical high-throughput omics study). This behavior allows it to overcome some of the limits of single-feature selection methods and provides a hard-thresholding approach at difference with projection-based variable selection methods. Certainly the combination evaluation is the most time-expensived step of the algorithm and it needs accurate algorithmic implementation for Big Data applications (see the next section for further information about the algorithm implementation strategy). The algorithm can be summarize as shown in 1.

```

Data: Data matrix (N, S)
Result: List of putative signatures
Divide the data into training and test by an Hold-Out method;
for couple  $\leftarrow (feature\_1, feature\_2) \in Couples$  do
    | Leave-One-Out cross validation;
    | Score estimation using a Classifier;
end
Sorting of the couples in ascending order according to their score;
Threshold over the couples score ( $K$ best couples);
for component  $\in connected\_components$  do
    | if reduction then
    |   | Iteratively pendant node remotion;
    | else
    |   | S
    | end
    | signature evaluation using a Classifier;
end
```

**Algorithm 1:** DNetPRO algorithm for Feature Selection.

So, given an initial dataset, that consists in  $S$  *samples* (e.g. cells or patients) each one described by  $N$  observations (our *variables*, e.g. gene or protein expression profiles), the signature identification procedure can be summarized with the following pipeline:

---

<sup>2</sup> A solution to a problem is classified as “overfitted” if small fluctuations on the data variance produces classification errors. This problem arises when the model perfectly fits the training set but it is not able to generalize to new (test) samples.

- separation of available data into a training and a test set (e.g. 33/66, or 20/80);
- estimation of the classification performance on the training set of all  $S(S - 1)/2$  variable couples through a computationally fast and reproducible cross-validation procedure (leave-one-out cross validation was chosen);
- selection of top-performing couples through a hard-thresholding procedure. The performance of each couple constitutes a *weighted link* of a network in which nodes are the variables connected at least through one link;
- every *connected component* in which the network is divided into constitutes an identified classification signature.
- (optional) in order to reduce the size of an identified signature, the pendant nodes of the network (i.e. nodes with degree equal to one) can be removed, in a single step or recursively until the core network (i.e. a network with all nodes with at least two links) is reached.
- all signatures are applied onto the test set to estimate their performances.
- a further cross validation step is performed (with a further dataset splitting into test and validation sets) to identify the best performing signature.

We would stress that this method is completely independent to the choose of the classification algorithm, but from a biological point of view a simple one is preferred to preserve an easy interpretability of the results. The geometrical simplicity of the resulting class-separation surfaces, in fact, allows an easier interpretation of the results, as compared to very powerful but black-box methods like nonlinear-kernel SVM or Neural Networks. Moreover the network interaction of variables can keep an internal ranking score of features importance or possible features cooperation. These are the reasons that move us to use very simple classifier methods in our biological application as diag-quadratic Discriminant Analysis or Quadratic Discriminant Analysis (Appendix A for more information about the mathematical background and implementation in the different languages). Both these methods allow fast computation and an easier interpretation of the results. This linear separation might not be common in some classification problems (e.g. image classification) but it is very plausible in biological systems, in which many responses to perturbation consist in an increase or decrease of variable values (e.g. expression of genes or proteins, see Fig. 1.1(b)).

In a general classification problem (e.g. image analysis) this could not be the case, since complex non linear separating surfaces may exist among the classes, but we hypothesize (and our results seem to confirm so) that in classification problems based on biological data such as gene expression these situations are not so common. This assumption is very plausible for biological data, since genes are in general up- or down-regulated in order to modify their activity and protein and metabolites most of the times respond consequently.

A second direct gain by the couples evaluation is related to the network structure: the DNetPRO network signatures allow a hierarchical ranking of the features according to their centrality compared to possible Kbest signatures. This underlying network structure of the signature could suggest further methods for signature dimensionality reduction based on network topological properties to fit real application needs and it could help to evaluate the cooperation of the variables for the class identification.

In the end we remark that the discriminating signatures have a purely statistical relevance by being generated with a purpose of maximal classification performance, but sometimes the selected features (e.g. genes, DNA loci, metabolites) can be of clinical and biological interest, helping to improve knowledge on the mechanism associated to the studied phenomenon [1, 28, 6, 30].

## 1.2 Synthetic dataset benchmark

Standard feature selection algorithms evaluate the single-variable performances. Starting from the ranked variables according to their score, a signature is obtained selecting the top scorer ones according to an hard thresholding or by an iteratively add of variables until a desired output score is reached. This method is called  $K$ -best algorithm and it permits to filter the number of variables without any constrain on their mutual interaction or correlation. On the other hand, the proposed DNetPRO algorithm tries to extract the more statistically significant variables considering the interaction between them, i.e the combination of variable-pairs. Thus, while the  $K$ -best algorithm scaled according to the number of variables, the DNetPRO algorithm is more computational expensive and its usage can be justify only if its efficiency can be proved.

We developed a toy model simulation to compare the performances of the standard  $K$ -best algorithm with the DNetPRO one, considering either the number of samples either the number of variables. Since the DNetPRO algorithm was designed to gene expression dataset applications, our toy model should consider a large number of variables with only a relative small number of samples. To simulate a so like synthetic dataset we used the toy model generator provided by the [scikit-learn package](#). This model generator allows to set a precise number of classes and distinguish between *informative features*, i.e. features which easily separate the class populations, and *redundant features*, i.e. features which represent noise in our problem. The number of informative features should be realistically small compared to the noise, so in our simulations we chose to introduce a maximum of 1% informative features in each simulation.

We randomly generated data from Gaussian distributions with an increasing number of samples and variables, i.e dimensions. In each simulation we split the number of samples in training and test sets (Hold-Out method, with 2/3 of data as training and 1/3 as test) and we applied the DNetPRO algorithm. From each simulation the extracted signatures were tested against the test set and the best performing one was kept. On the same data we applied the  $K$ -best algorithm and we kept the same number of variables of the DNetPRO best signature, i.e  $K$  equal to the number of nodes in the DNetPRO best signature. In this way we can compare the performances obtained on the test set by the two methods. We would highlight that, in general, there is not a stop criteria on the  $K$ -best algorithm, so the number of variables selected could be smaller or greater than the number of DNetPRO signature nodes. However, we can reasonably assume that according to the  $K$ -best interpretation the selected features should be the most performing ones and adding more variables should introduce only small quantity of noise. This justify the use of the same number of variables between the two algorithms using the DNetPRO signature as reference. In Fig. 1.2 we show the results obtained in our simulations: the results are obtained keeping fixed the number of variables/samples and varying the number of samples/variables, Fig. 1.2(a) and Fig. 1.2(b) respectively.

For the same number of variables (Fig. 1.2(a)) we can noticed as the two methods performs quite similarly but the DNetPRO is able to reach better performances as the number of samples increase.

This trend can be explained also in statistical terms: with small samples the variability of our (random) data is large and so the performance distributions is more unstable. With a greater number of samples, the variances of our classes is reduced and also the statistical quantities involved in the computation of the discriminant curve can be evaluated with more accuracy. As the number of samples increase, the statistically evaluation of the variables becomes easier and increases the correspondence between the top scorer variables and the true-informative ones. In low sample cases, the quantity of noise is bigger and in an high dimensional space is harder to find the most informative directions and also noise variables could reach performances higher than informative ones.

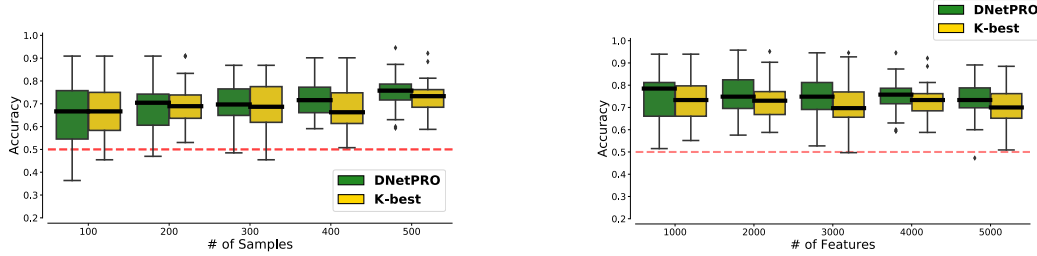


Figure 1.2: Synthetic dataset simulation. Comparison of accuracy performances obtained by the DNetPRO algorithm and the  $K$ -best algorithm. (a - left) Performances obtained in function of the number of samples, keeping fixed the number of variables. (b - right) Performances obtained in function of the number of variables, keeping fixed the number of samples.

Despite of the simplicity of our toy model, the DNetPRO is able to highlight its efficiency in terms of performances against the single-feature method.

A slight different behavior is shown by varying the number of variables and keeping fixed the number of samples (Fig. 1.2(b)). In this case we have that the median accuracy (black line in the plot) is always higher for the DNetPRO algorithm. With a small number of variables (left part of the plot) the  $K$ -best algorithm performances are more stable and, only from a statistical point-of-view, we can justify the efficiency of the DNetPRO algorithm (the median of the distribution is still higher compared to the  $K$ -best one). As the number of variables increases, also the efficiency of the DNetPRO algorithm increases until it exceeds the  $K$ -best algorithm (and its distribution is narrowed). We reached this situation quite faster in our simulation since we constrained our toy model with a forced unbalance between the number of samples and variables, i.e the so-called ill-posed problems. The DNetPRO was designed to work in this situations and it is able to reach high accuracy results also in critical ill-posed problems. The evaluation of pair of variables could be helpful to find good variables which are penalized in the single score ranking, but which can demonstrate a good performance-interaction with other variables. In this cases, the DNetPRO results could be helpful also to understand the variable interactions, due to the network structure of the signature that can bring to deeper considerations on the fine grain interaction of the variables in a real problem context.

This kind of toy model is considered a standard for feature extraction algorithm testing but it puts several disadvantages for the DNetPRO evaluation. We started our discussion about the DNetPRO taking into account the two distributions of data showed in Fig. 1.1(a). The DNetPRO algorithm was designed to face on that kind of situations in better way. The limits of our algorithm are so bounded to the sample distributions: if the informative variables are totally independent one from each other, the couples evaluation does not guarantee the best approach to the problem. An informative variable could work better with noise data than with another informative one: in this way we could expect a star-network signature, in which the central node would be the informative variable connected to a series of noise variables. Considering the signatures extracted by the DNetPRO algorithm we noticed this kind of behavior: the core of our signatures was principally composed by informative variables (which were manually introduced so easily traced).

We have to face on also the problem of multiple putative (disjointed) signatures: the DNetPRO algorithm takes into account only the connected components with the highest score as putative signature. If the informative variables are disjointed, the corresponding star-networks will be disjointed until a common noise-variable creates a bridge between the two connected components. This means that we have to enlarge the amount of nodes in our signature and thus increase the difficulty in the filtering of noise.

We evaluated both these situations in our toy model simulations. In the first case, we introduced only two informative variables obtained by a sampling of the distribution showed in Fig. 1.1(a). In all our simulations, the DNetPRO algorithm was able to identify the couple of these variables as best putative signature. At the same time the  $K$ -best algorithm find with more difficulty those variables, especially when the number of variables become greater. Considering the distribution of single-variable scores, in fact, we could noticed as the informative variables, despite they are manually introduced, were not always the top scoring ones: in large dimensional spaces also noise-variables produced high(er) performances.

Using the same sample distributions for informative features, we manually introduced multiple couples in our dataset. As expected the DNetPRO algorithm is not able to identify in a single connected components, and thus a single putative signature, the full set of informative variables, while the  $K$ -best algorithm easily find them in the top scoring ranking. To guarantee the full set of informative features into the DNetPRO signature, we had to enlarge the number of nodes and thus we had to introduce multiple noise-variables. This highlights the limits of the DNetPRO algorithm and also the need of a (optional) filter procedure to apply to the putative signatures for these critical cases<sup>3</sup>.

## 1.3 Algorithm implementation

The DNetPRO algorithm is made by a sequence of different steps which have to be performed sequentially for a signature extraction. For this purpose, each step can be optimized independently by using the full set of available computational resources<sup>4</sup>. In this section it will be analyzed each part of the pipeline focusing on the optimization strategies used for the algorithm implementation.

The full code is open source and available at [8]. The code installation is automatically tested using [travis](#) (for Linux and MacOS environments) and [appveyor](#) (for Windows environments) at every commit. The installation can be performed using [CMake](#) and a full set of installation instructions can be found in the on-line project documentation.

The [Python](#) version of the algorithm (see next sections) can be installed via [setup.py](#) and the compilable parts of it checked via [CMake](#). The [Python](#) installer provides also the full list of dependencies of the project, which will be automatically installed by the main.

In the Github repository, it can be found also a full list of example scripts and utilities to obtain the results showed in the next sections. We provide also the complete benchmark pipeline used in our simulation and able to run on cluster environment using the [SnakeMake](#) version of it (see next section).

### 1.3.1 Combinatorial algorithm

The most computational time-expensive step of the algorithm is certainly the couples evaluation. From a computation point-of-view this step requires ( $O(N^2)$ ) operations for the full set of combinations. Since we want to perform also an internal Leave-One-Out cross validation for the couple performances estimation, we have to add a ( $O(S - 1)$ ) to the algorithmic complexity. Let's focused on some preliminary considerations before the implementation discussion:

---

<sup>3</sup> In the algorithm description we discussed about the possibility of removing pendant nodes as optional filter procedure. In the case described above this step can help but not completely solve the problems: if there are two disjointed signatures we have to enlarge the number of nodes until we create a connection between them but this connection would be probably due to a noise variable. The pendant nodes remotion can help to reduce the amount of node but the link which connects the two components would be preserved.

<sup>4</sup> Further optimization can be performed in a cross validation environment and they will be discussed later in this section.

- **Performances:** we aim to apply our method on large datasets since we have to focused on time performances of the code and particularly on this step (identified as bottleneck). To reduce as much as possible the call stack inside our code, we should perform the entire code with the small number of functions as preferably and possibly inside a unique main. Moreover we can simplify the for loop and take care of the automatic code vectorization performed by the optimizer at compile time (SIMD, *Single Instruction Multiple Data*). A further optimization step to take in count is related to the cache accesses: the use of custom objects inside the code should benefit from cache accesses (AoS vs SoA, *Array of Structure vs Structure of Arrays*).
- **Interdependence:** the variable couple performances evaluation is a completely independent computational process and can be faced on as  $N^2$  separately tasks. Thus it can be easily parallelizable to increase speed performance.
- **Simplify:** the use of simple classifier for performance evaluation simplify the computation and the storage of the relevant statistical quantities. In the discussed implementation we focused on a Diag-Quadratic classifier (see Appendix A for further information) in which only means and variances of the data plays a role in its evaluation.
- **Cross Validation:** the use of Leave-One-Out cross validation allows to perform substantially optimizations in the statistical quantities evaluations across the folds (see discussion in Appendix A - Numerical Implementation).
- **Numerical stability:** we have also to take in care the numerical stability of the statistics since we are working in the assumption of a reasonable small number of samples compared to the amount of variables. This behavior particularly affects the variance estimation: the chose of a numerical stable formula for this quantity play a crucial role for the computation because the classifier score has to be normalized by this.

With these ideas in mind we can write a C++ code able to optimize this step of computation in a multi-threading environment with the purpose of testing its scalability over multi-core machines.

Starting from the first discussed point, we chose to implement the full code inside a unique main function with the help of only a single SoA custom object and one external function (*sorting algorithm* discussed in the next section). This allows us to implement the code inside a single parallel section reducing the time of thread spawns. We chose to import the data from file in sequential mode since the I/O is not affected by parallel optimizations.

Following the instructions suggested in Appendix A - Numerical Implementation, we compute the statistic quantities on the full set of data before starting the couples evaluation. Taking a look to the variance equation

$$\sigma^2 = \frac{\sum_{i=1}^S (x_i - \mu)^2}{S - 1} = \frac{\sum_{i=1}^S (x_i^2)}{S - 1} - \mu^2$$

we can see that the first equation involve the computation of the mean as a simple sum of the elements but a large number of subtractions from it that are numerical unstable for data outliers (moreover because they are elevated to square). The better choice in this case is given by the second formulation that allows us to compute the both quantities in

the formula inside a single parallel loop<sup>5</sup>. At each cross validation we will use the two pre-calculated sums of variables removing the only data point excluded by the Leave-One-Out. Another precaution to take in care is to add a small epsilon to the variance before its use at denominator inside the classifier function to prevent numerical underflow.

The main role is still given by the couples loop. The set of pair variables can be obtained only by two nested for loops in C++ and naive optimization can be simply obtained by reducing the number of iterations following the triangular indexes of the full matrix (by definition the score of the couple  $(i, j)$  is equal to the score of  $(j, i)$ ). This precaution easily allows the parallelization of the external loop and drastically reduce the number of iteration, but it also creates a link between the two iteration variables. The new release of OpenMP libraries [11]<sup>6</sup> (from OpenMP 4.5) introduce a new *keyword* of the language that allows the collapsing of nested for loops in a single one (whose number of iterations is given by the product of the single dimensions), in the only exception of completely independences of iteration variables. So the best strategy to use in this case is to perform the full set of  $N^2$  iterations with a single `collapse` clause in the external loop<sup>7</sup>.

Listing 1.1: Python parallel couples evaluation algorithm

```

1 import pandas as pd
2 import itertools
3 import multiprocessing
4 from functools import partial
5
6 from sklearn.naive_bayes import GaussianNB
7 from sklearn.model_selection import LeaveOneOut, cross_val_score
8
9 def couple_evaluation (couple, data, labels):
10    f1, f2 = couple
11
12    samples = data.iloc[[f1, f2]]
13    score = cross_val_score(GaussianNB(), samples.T, labels,
14                           cv=LeaveOneOut(), n_jobs=1).mean() # nested
15    parallel loops are not allowed
16
17    return (f1, f2, score)
18
19 def read_data (filename):
20    data = pd.read_csv(filename, sep='\t', header=0)
21    labels = data.columns.astype('float').astype('int')
22    data.columns = labels
23
24    return (data, labels)
25
26 if __name__ == '__main__':
27
28    filename = 'data.txt'
29
30    data, labels = read_data(filename)
31
32    Nfeature, Nsample = data.shape
33
34    couples = itertools.combinations(range(0, Nfeature), 2)
35    couples_eval = partial(couple_evaluation, data=data, labels=labels)

```

---

<sup>5</sup> To facilitate the SIMD optimization the code is written using only float (single precision) and integer variables. This precaution takes in care the register alignment inside the loops and facilitate the compile time optimizer.

<sup>6</sup> The OpenMP library is the most common non-standard library for C++ multi-threading applications.

<sup>7</sup> Obviously the iteration where the inner loop variable is lower than the outer one will be skipped by an if condition.

```

36     nth = multiprocessing.cpu_count()
37
38     with multiprocessing.Pool(nth) as pool:
39         score = zip(*pool.map(couple_eval, couples))

```

In this section we also provide an “equivalent” Python implementation with the use of common machine learning libraries and parallel settings (ref. 1.1). In the next sections we will discuss the computational performances of this naive implementation with C++ one discussed above.

### 1.3.2 Pair sort

The sorting algorithm starts at the end of variable couple evaluation and re-order the pairs in ascending order to ease the next steps of signature identification<sup>8</sup>. This step is performed in the same code (and same parallel section) of the previous section but it deserves an own topic for a better focus on the parallelization strategy chosen. Moreover, there are many common parallel implementation of sorting algorithm and, to reach the best performances, we have to chose the appropriated one.

The sorting algorithm are already implemented in serial version in the major part of the languages (Python and C++ included). The naive version of the algorithms are also quite optimized and they perform the computation with complexity ( $O(N \log(N))$ )<sup>9</sup>. In this case we have not to re-invent any sorting technique but only insert as well as possible these algorithms inside a parallel sections and use the variable format chosen for couple performances storage. Since we are working with SoA objects we need to re-order all the structure arrays in the same way. So we can not use a simple sort function but can compute the set of indexes that allow the re-order of the arrays, the so called `argsort` method. To rearrange the indexes according to a given array of values we can use the templates in C++.

As parallelization strategy we can yet invoke the new *keywords* of OpenMP libraries and apply a *divide-and-conquer* architecture using a tree of independent `tasks`<sup>10</sup>. Using the maximum power of two of the available threads, we split the computation in equal size sub-arrays and perform independent `argsorts`. Then, going backwards to the subdivisions at each step, we merge the sub-arrays two-by-two until the root (ref Fig. 1.3).

### 1.3.3 Network signature

After the rearrangement of feature pairs in ascending order we can start to create the variable network and looking for its connected components as putative signatures. Each feature will be represent a node in the network and a given pair will be a connection between them. Since the full storage of the network would require a matrix ( $N \times N$ ), we have to chose a better strategy for the processing<sup>11</sup>.

---

<sup>8</sup> We are talking about couples performances meaning the classification accuracy of the feature pair up to now. In some cases the simple accuracy is useless, especially when we are working with unbalanced population classes. In this case we can use a statistical score which takes in count the balanced between the right classifications of our samples (e.g Matthews Correlation coefficient, MCC). The developed code evaluate either the global accuracy of classification either the MCC and, with slight changes allows to perform the re-ordering of feature pair according to the desired score. Since in the next section we will discuss the application of the DNetPRO algorithm to real data using only the classification accuracy as score, we focused only on it in the next sections.

<sup>9</sup> We are considering only un-stable sort in which the preserving order of equivalent elements in the array is not guaranteed.

<sup>10</sup> Tasks in OpenMP are code blocks that the compiler wraps up and makes available to be executed in parallel.

<sup>11</sup> We are working in the hypothesis of very large  $N$ .

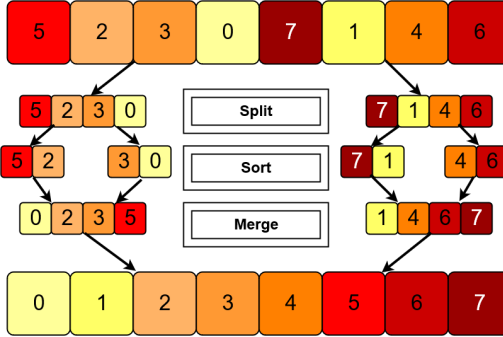


Figure 1.3: Parallel merge-sort algorithm scheme. Starting from the original array, the master thread splits the work (sub-arrays) along two slave threads (**split** step in the graph). The split recursion is applied until a required size of sub-arrays is reached. Each slave-thread applies a sort function (**sort** step in the graph). Then, the full array is recombined following back the thread recursion and applying an **inplace-merge** function (**merge** step in the graph).

The ordered set of couples computed in the previous section represents a so-called *COO sparse matrix* (Coordinate Format sparse matrix) and we can reasonable assume that the desired signature will be composed by the top ranking of them. So, the first step will be to cut a reasonable percentage of the full set of pairs and process only them.

Moreover, we are interested in a small set of variables unknown a prior. The load of all the node pairs into the same graph can slow down the computation. An iterative method (with stop criteria) can perform better in the large case of samples and only in worst cases the full set of pair will be loaded.

Since the described algorithm step does not require particular performance efficiency now, the main code used in our simulation was written in pure Python. A C++ implementation of the same algorithm was developed with the help of the Boost Graph Library [29] (BGL), but to not overweight the code installation, it was reserved just for a style exercise. In this section we discuss about this second version and also about the strategies chosen to implement an efficiency version of it. This version of the algorithm was also used as stand alone method for other applications that will be presented later.

BGL is a very wide framework for graph analysis based on template structures. The library efficiency discourage the users to re-implement the same algorithms and, for the current purposes, it was resulted more than sufficient.

Starting from the top scorer feature pairs, we progressively add each couple of nodes to an empty graph. At each iteration step, the number of connected components is evaluated until a desired number of nodes (greater or equal) is not reached<sup>12</sup>. Two degree of freedom are left to the user: in order, **pruning** and **merging**. The first one performs an iteratively remotion of nodes with degree equal (or lower) than 1, i.e pendant nodes, until the graph core is not filtered. The **merging** clause choose between the biggest connected component or the the set of all the disjoint connect components as putative signature. The output of **merging** step determine the number of nodes in the graph which have been considered for the stop criteria.

A crucial role in the optimization of the algorithm is played by the chosen BGL graph structure. Since the two degree of freedom imply a continuous rearrangement of the graph nodes, the strategy chosen is to apply a filter mask over the main graph structure that highlights the only part of interest. This can be done using the `boost :: filtered_graph`

<sup>12</sup> This procedure is quite similar to put a threshold value on the couple performances or just simpler highlight inside the full network the components linked by weights greater than a given value.

object of BGL. In 1.2 the C++ snippet is shown.

Listing 1.2: DNetPRO signature extraction

```

1 #include <boost/graph/adjacency_list.hpp>
2 #include <boost/graph/connected_components.hpp>
3 #include <boost/graph/filtered_graph.hpp>
4 #include <boost/function.hpp>
5 #include <boost/graph/iteration_macros.hpp>
6
7 typedef typename boost :: adjacency_list< boost :: vecS, boost :: vecS,
8     boost :: undirectedS, boost :: property< boost :: vertex_color_t, int >,
9     boost :: property < boost :: edge_index_t, int > > Graph;
10
11
12 std :: vector < int > FeatureSelection (int ** couples, const int &
13 min_size, bool pruning=true, bool merging=true)
14 {
15     Graph G;
16     std :: set < V > removed_set;
17     Filtered Signature (G, boost :: keep_all {}, [] (V v) {return removed_set
18         .end() == removed_set.find(v);});
19
20     int L = 0, leave, Ncomp, i = 0;
21
22     while ( true ){
23
24         boost :: add_edge (couples[i][0], couples[i][1], G);
25
26         while ( pruning ){
27
28             leave = 0;
29             BGL_FORALL_VERTICES (v, Signature, Filtered);
30             if ( boost :: in_degree (v, Signature) < 2 ){
31                 removed_set.insert (v);
32                 ++ leave;
33             }
34
35             if ( leave == 0 )
36                 break;
37         }
38
39         if ( num_vertices (G) - removed_set.size() ){
40
41             components.resize (num_vertices (G));
42
43             Ncomp = boost :: connected_components (Signature, &components[0]);
44
45             if ( merging ){
46
47                 BGL_FORALL_VERTICES (v, Signature, Filtered)
48                 if ( boost :: in_degree(v, Signature) )
49                     core.push_back ( static_cast < int >(v) );
50             }
51             else {
52
53                 std :: map < int, int > size;
54                 for ( auto && comp : components ) ++ size[comp];
55
56                 auto max_key = std :: max_element (std :: begin(size), std :: end(
57                     size));

```

```

55                                     [] (const decltype(size) :: 
56     value_type && p1, const decltype(size) :: value_type && p2)
57                                         { return p1.second < p2.second;
58 } ->first;
59
60     BGL_FORALL_VERTICES (v, Signature, Filtered)
61         if (components[v] == max_key)
62             core.push_back( static_cast < int >(v));
63     }
64
65     components.resize (0);
66     L = static_cast < int >(core.size());
67 }
68
69     removed_set.clear();
70
71     if (L >= min_size) break;
72
73     ++ i;
74
75     core.resize (0);
76 }
77
78     return core;
79 }
```

In the above description, it should be clear that, given any set of ordered (in ascending order) couples of variables, this algorithm allows to extract the core network independently by the procedure which generate them. So it can be used as dimensionality reduction algorithm of general purpose network structures. An example of this kind of application was reported in Appendix B - Venice Road Network in which we summarized the results of [24, 10].

### 1.3.4 DNetPRO in Python

Up to now we are focusing on the algorithm performances, leaving out the usability of the DNetPRO algorithm for the (research) community. Despite the C++ is one of the most efficient and old programming language<sup>13</sup>, the Python language users are increasing in the last few years. Python is becoming a leader in scientific research publications and the large part of Machine Learning analysis are performed using Python libraries (in particular scikit-learn library). So we have to reach a compromise between the performances and usability of new developed codes and it can be reached using the Cython [3] framework.

Cython “language”<sup>14</sup> allows an easy interface between C++ codes and Python language. With a relatively simple wrapping of the C++ functions, they can be used inside a pure Python code preserving as much as possible the computational performances of the pure C++ version. In this way we can create a simple Python object which performs the full set of DNetPRO steps and, moreover, which is compatible with the functions provided by the other machine learning libraries.

With this purposes we chose to operate a double wrap of the C++ functions to separate as much as possible the C++ component from the Python one<sup>15</sup>. The Python object was

---

<sup>13</sup> Still in common use in scientific research groups.

<sup>14</sup> It is not a real programming language since it is based on Python. However it has its own syntax and keywords which are different either from Python either from C++. In the end it needs a compiler to run and it is certainly different from Python.

<sup>15</sup> Cython wrap are very powerful tools for C++ integration into Python code but, by experience, they are difficult to manage by pure-Python users. A simple workaround is to perform a first wrap of the C++ function inside a Cython object and a second wrap of it into a pure-Python one. This two-steps wrap certainly gets worse the computational performances but it allows a complete separation between the

written considering a full compatibility with the `scikit-learn` library to allow the use of the DNetPRO feature selection as an alternative component of other Machine Learning pipelines.

### 1.3.5 DNetPRO in Snakemake

The starting (silent) hypothesis done until now is that we are running the DNetPRO algorithm on a single dataset (or better on a single Hold-Out subdivision of our data). On this configuration it is legal to stress as much as possible the available computational resources and parallel processing each step of the algorithm.

If we want to introduce our algorithm inside a larger pipeline, in which we compare the resulting obtained over a Cross-Validation of our datasets we have to re-think about the parallelization done. In this case, each fold of the cross validation can be interpreted as an independent task and, following the main programming rule “*parallelize the outer, vectorize the inner*”, we should spawn a thread for each fold and perform the couple evaluation in sequential mode. Certainly, the optimal solution would be to separate our jobs across a wide range of inter-connected computers and still perform the same computation in parallel but it would required to implement our hybrid (C++ and Python) pipeline in a Message Passing Interface (MPI) environment.

An easier solution to overcome all these problems can raise by the use of `SnakeMake` [18] rules. `SnakeMake` is an intermediate language between `Python` and `Make`. Its syntax is almost like the `Make` language, but with the help of the easier and powerful `Python` functions. It is widely used for bioinformatic pipeline parallelization since it can easily applied over single or multi-cluster environment (master-slave scheme) with a simple change of command line.

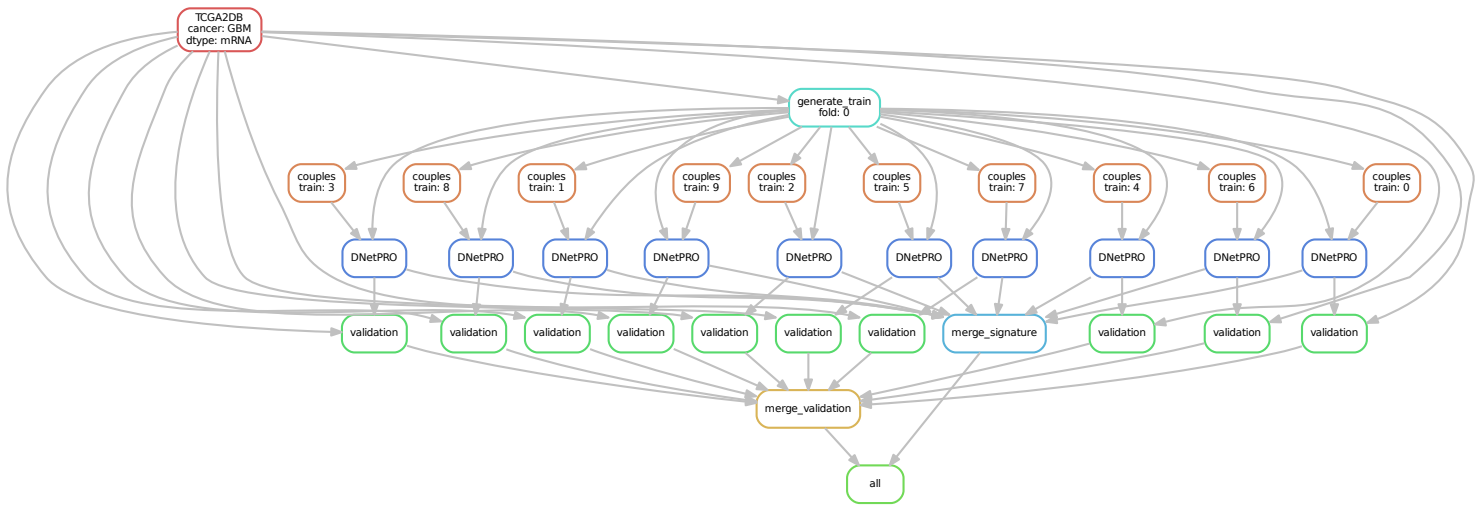


Figure 1.4: Example of DNetPRO pipeline on a single cross validation. It is highlighted the independence of each fold from each other. This scheme shows a possible distribution of the jobs on a multi-threading architecture or for a distributed computing architecture. The second case allows further parallelization scheme (hidden in the graph) for each internal step (e.g. the evaluation of each pair of genes).

---

compiled part of the code (Cython) and the interpreted (Python) one. Moreover we can leave back all the checks on input parameters in the C++ version since they will be performed at run time in the Python wrap.

So to improve the scalability of our algorithm we implement the benchmark pipeline scheme using Snakemake rules and a work-flow example for a single cross-validation is shown in Fig. 1.4. In this case each step of Fig. 1.4 can be performed by a different computer unit preserving the multi-threading steps, with a maximum scalability and the possibility to enlarge the problem size and the number of variables.

### 1.3.6 Time performances

As described in the above sections, the DNetPRO is a combinatorial algorithm and thus it requires a particular accuracy in the code implementation to optimize as much as possible the computational performances. The theoretical optimization strategies, described until now, have to be proved by quantitative measures.

We tested the computational performances of our **Cython** (**C++ wrap**) implementation against the pure **Python** (naive) implementation shown in 1.1. The time evaluation was performed using the **timing** Python package in which we can easily simulate multiple run of a given algorithm<sup>16</sup>. In our simulations, we monitored the three main parameters related to the algorithm efficiency: the number of samples, the number of variables and (as we provided a parallel multi threading implementation) the number of threads used. For each combination of parameters we performed 30 runs of both algorithms and we extracted the minimum execution time. The tests were performed on a classical bioinformatics server (128 GB RAM memory and 2 CPU E5-2620, with 8 cores each). The obtained results are shown in Fig. 1.5. In each plot, we fixed two variables and we evaluated the remaining one.

In all our simulations, the efficiency of the (optimized) Cython version is easily visible and the gap between the two implementations reached more than  $10^4$  seconds. On the other hand, it is important to highlight the scalability of the codes against the various parameters. While the code performances scales quite well with the number of features (Fig. 1.5(a)) in both the implementations, we have a different trend varying the number of samples (Fig. 1.5(b)): the **Cython** trend starts to saturate almost immediately while the computational time of the **Python** implementation continues to grow. This behavior highlights the results of the optimizations performed on the **Cython** implementation which allows the application of the DNetPRO algorithm also to larger datasets without loosing performances. An opposite behavior is found monitoring the number of threads (ref Fig. 1.5(c)): the **Python** version scales quite well with the number of threads<sup>17</sup>, while **Cython** trend is more unstable. This behavior is probably due to a not optimized schedule in the parallel section: the work is not equally distributed along the available threads and it penalizes the code efficiency creating a bottleneck related to the slowest thread. The above results are computed considering a number of features equal to 90 and, thus, the parallel section distributes the 180 ( $N \times N$ ) iterations along the available threads: when the number of iterations is proportional to the number of threads used (12, 20 and 30 in our case), we have a maximization of the time performances. Despite of this, the computational efficiency of the **Cython** implementation is much better than the **Python** one, of which the usage is indisputable.

---

<sup>16</sup> We would stress that we can use the **timing** Python package only because we provided a **Cython** wrap of our DNetPRO algorithm implementation. We would also highlight that, albeit minimal, the **Python** superstructure penalizes the computational performances and the best results can be obtained using the pure **C++** version of the code.

<sup>17</sup> The optimal result should be a linear scalability with the number of threads but it is always difficult to reach this efficiency. Thus, a reasonable good result is given by a progressive decrease with increasing the number of threads.

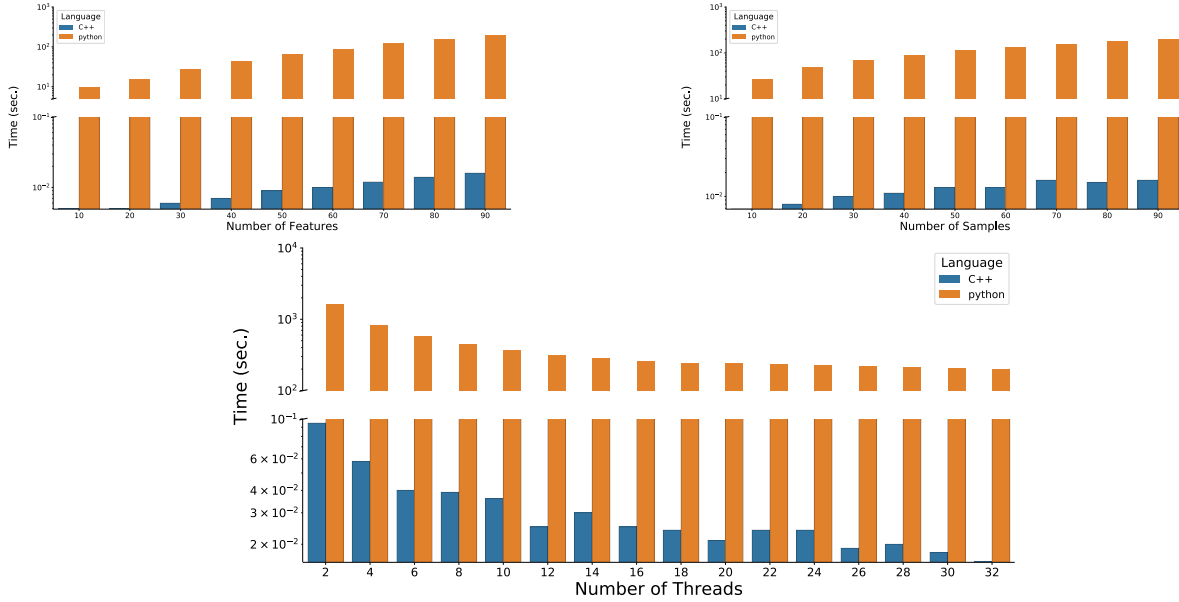


Figure 1.5: Execution time of DNetPRO algorithm. We compare the execution time between pure-Python (orange) and Cython (blue, C++ wrap) implementation. **(a - left)** Execution time in function of the number of variables (the number of samples and the number of threads are kept fixed). **(b - right)** Execution time in function of the number of samples (the number of variables and the number of threads are kept fixed). **(c - bottom)** Execution time in function of the number of threads (the number of variables and the number of samples are kept fixed).

## 1.4 Benchmark of DNetPRO algorithm

Up to now we have been talked about the DNetPRO algorithm from a theoretical point-of-view. Starting from this section, we discuss about the application of the algorithm on real biological datasets (see Appendix B - Venice Road Network for results obtained on a different kind of data).

Despite of previous version of the DNetPRO method were already applied on biological data [1, 28, 6, 30], a wide range benchmark of it was still missing. In the following sections we describe the results obtained on the Synapse dataset and published in [9].

### 1.4.1 Synapse dataset

As benchmark dataset was chosen the core sets extracted from the The Cancer Genome Atlas (accession number [syn300013](#), doi:[10.7303/syn300013](#)) (*Synapse dataset* in the following), used in a previous study [31] which aimed at quantifying the role of different omics data types (e.g. mRNA and miRNA microarray data, protein levels measured with Reverse Phase Protein Array - RPPA) via different state-of-the-art classification methods. This allowed us to compare our results to a large set of commonly used classification methods, by using their performance validation pipeline (accession number [syn1710282](#), doi:[10.7303/syn1710282](#)).

The Synapse dataset is composed by four tumors datasets: kidney renal clear cell carcinoma (KIRC), glioblastoma multiforme (GBM), ovarian serous cystadenocarcinoma (OV) and lung squamous cell carcinoma (LUSC). For each cancer type we applied the DNetPRO algorithm on mRNA, miRNA and RPPA data and we compare the performances results with the Yuan et al. ones.

The summary description of the datasets used is reported in the Tab. 1.1.

Cancer	mRNA	miRNA	Protein	Number of samples
GBM	AgilentG4502A 17814	H-miRNA_8x15k 533	RPPA <sup>a</sup>	210
	HiseV2 20530	GA+Hiseq 1045	RPPA 166	243
OV	AgilentG4502A 17814	H-miRNA_8x15k 798	RPPA 165	379
	HiseqV2 20530	GA+Hiseq 1045	RPPA 174	121
LUSC				

Table 1.1: In the first row platforms are reported and the second shows the dimension of dataset as number of probes. AgilentG4502A: Agilent 244K Custom Gene Expression G4502A; HiseqV2: Illumina HiSeq 2000 RNA Sequencing V2; H-miRNA\_8x15K: Agilent 8 × 15K Human miRNA-specific microarray platform; GA+Hiseq: Illumina Genome Analyzer/HiSeq 2000 miRNA sequencing platform; RPPA: MD Anderson reverse phase protein array. The last column shows the number of sample.

<sup>a</sup> Missing data-type for that cancer type.

Each tumor dataset was pre-processed by adding a zero-mean Gaussian random noise ( $\sigma = 10^{-4}$ ) to remove the possible null values in the database, which could produce numerical errors in the distances evaluation between genes. Then, we randomly split each dataset in training and test sets with a stratified (i.e. balanced for class sample ratio) 10-fold procedure: with the stratification we are reasonably sure that each training-set is a good representative of the whole sample set. The choice of a 10-fold splitting is aimed to reproduce the analysis pipeline presented by Yuan et al. with an analogous cross-validation procedure. Since we don't have exact details of their data splitting, the cross validation was repeated 100 times, for a total of 1000 training procedures for each tumor (OV, LUSC, KIRC, GB) and data type (mRNA, miRNA, RPPA). Each training procedure led to the extraction of multiple signatures.

We chose threshold values in order to obtain a resulting number of variables (network nodes) in the order of  $10^2 - 10^3$ , and identified all connected components of the network as signatures. If more than one component existed, each one was considered as a different signature.

The final multidimensional signatures were tested by a Discriminant Analysis with a diag-quadratic distance, to avoid possible problems about covariance matrix inversion (as for the Mahalanobis distance).

We remark that DNetPRO can provide more than one signature as a final outcome, given by all the connected components found in the variable network, or a unique top-performing signature can be obtained by a further cross-validation step (procedure *A* and procedure *B* in Fig. 1.6, respectively).

In the single cross validation configuration (procedure *A* in Fig. 1.6), the best signature was extracted as the one reaching the highest accuracy score during the training step. This best signature was then tested over the available test set.

When also the second cross validation was used (procedure *B* in Fig. 1.6) the best signature wasted as the most performing over a subset of the whole test set (*validation set*), and the final performance was evaluated on the remaining *scoring set*.

To compare our results with the work of Yuan et al., we used the AUC (*Area Under the Curve*) score, that they provided in the paper as the result of their analyses. The

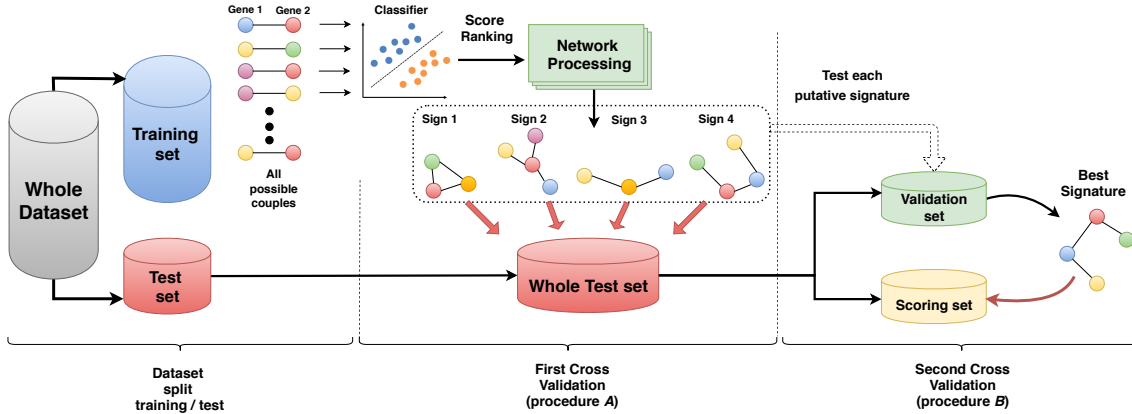


Figure 1.6: Scheme of DNetPRO algorithm. On the “training set”, all possible couples are used for Discriminant Analysis, generating the fully connected network weighted by classification performance. Thresholding ranked couples, several signatures can result (as connected components) and their performance is evaluated on the “whole test set” (procedure *A*). A unique best signature can be identified on a “validation set” and tested in a “scoring set”, obtained by further splitting the “whole test set” (procedure *B*).

distribution of our results could be compared to the single score value given in the other work.

#### 1.4.2 mRNA dataset

We applied both training procedure (ref. Fig. 1.6) on the mRNA dataset. The results are shown, as distribution of AUC (Area under the curve) score, in Fig. 1.7 (a) for the best signatures obtained with procedure *A* (corresponding to the validation approach used in [31]), while results with the full cross-validation procedure *B* are shown in Fig. 1.7 (b).

As expected, performances decrease with the introduction of the second cross validation step, but the values remain quite stable showing the robustness of the extracted signatures, and we remark that the validation procedure used in the reference paper by Yuan et al. resembles our approach without the second validation step.

All results are comparable (LUSC) or better (KIRC, GBM) than the results reported in [31], except for the OV dataset, also with the more conservative approach involving a further cross-validation step. The size of the extracted signatures is quite constant, and smaller than 500 genes in each pipeline execution.

To test the robustness of our method, since each cross-validation procedure may generate different signatures, we measured the overlap of the genes belonging to each mRNA signature over 100 simulations with different training-test data splitting. We observed an average overlap ranging from 40% to 60%, with a smaller group of genes found across all the 100 cross-validation iterations.

In this application the DNetPRO algorithm has several advantages: easy scalability on parallel architectures, simple signature interpretation allowing a valuable application in a biomedical context and a significant robustness in a highly noisy environment such as genomics measurements.

#### 1.4.3 miRNA and RPPA dataset

The same analysis pipeline presented in the paper about gene expression data from the Synapse dataset is applied in this Section also to the miRNA and RPPA datasets, with

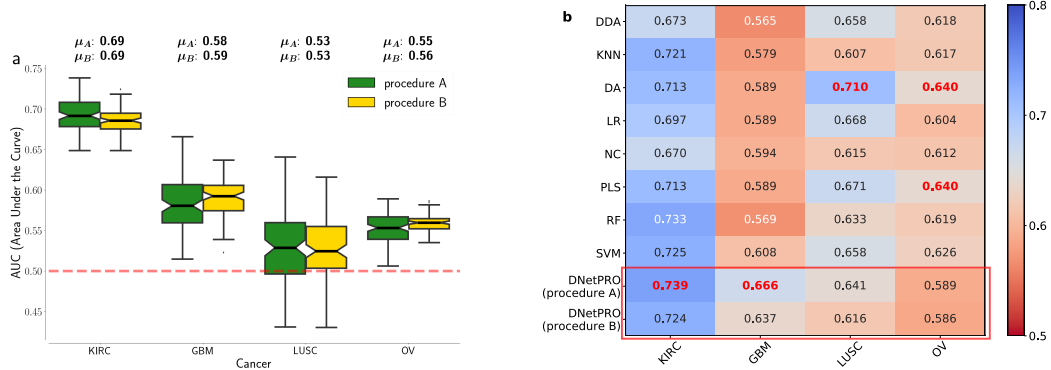


Figure 1.7: Results obtained by the DNetPRO algorithm pipeline on four mRNA tumor datasets, as from the Synapse database [31]. (a) Distributions of AUC values for the tumor datasets. Green boxplots: results using procedure *A* as described in Fig. 1.6; yellow boxplots: results obtained using procedure *B*. (b) Comparison of DNetPRO results with the methods used in the paper of Yuan et al.: max AUC values obtained over the 10-Fold cross-validation procedure.

the results presented in Fig. 1.8.

The results obtained on the miRNA dataset (Fig. 1.8 (a, b)) are comparable to the reference, while for the RPPA dataset only the LUSC tumor shows AUC values comparable with the others. Moving from the procedure *A* to the procedure *B*, i.e. adding a second cross-validation step, the RPPA performances drastically decrease for the KIRC and OV, while their remain quite stable for the LUSC dataset. The same behavior is shown in the miRNA datasets in which however both performances are still comparable or better (KIRC, GBM, LUSC) than the reference ones.

These results are not so good as the mRNA ones and this behavior highlights some limitations of the algorithm. In the mRNA dataset we hypothesized a monotonic behavior of genes (up- or down-regulation of gene expression level) and this model is very likely. An analogous model for the miRNA data has not yet been demonstrated. We can guess that the low performances obtained on the RPPA were related to the intrinsic nature of these data and to the experimental difficulties about data interpretation. We have to consider also the technique used to acquire these kind of data which is different from the mRNA one: different experiments can introduce different noise sources which can affect our model performances.

#### 1.4.4 Couple ranking

Since the number of variable pairs is typically very large (e.g.  $10^8$  pairs with gene expression microarrays containing about  $10^4$  probes), many of them may achieve the same performance, since the possible performance values are integer number typically in a limited range (corresponding to the number of available samples,  $10^2 - 10^3$  in many cases). Therefore, the ranking of pairs by their performance is characterized by multiple “plateaus” (Fig. 1.9(a)), and the selection of probe pairs, based on a hard thresholding procedure, is highly influenced by this feature. Monitoring this trend behavior can be noticed that only a few number of pairs belongs to the first performances chunks and, while the performances decrease, multiple pairs and features appear, as it can be seen in Fig. 1.9(a).

This kind of trend highlight the difficulty on finding informative features inside the huge noise of other variables and it gives us a constrain in the developing of a realistic biological toy model. Moreover, it confirms us that a putative signature could be made by only a few amount of central genes at least weakly connected with other noise nodes.

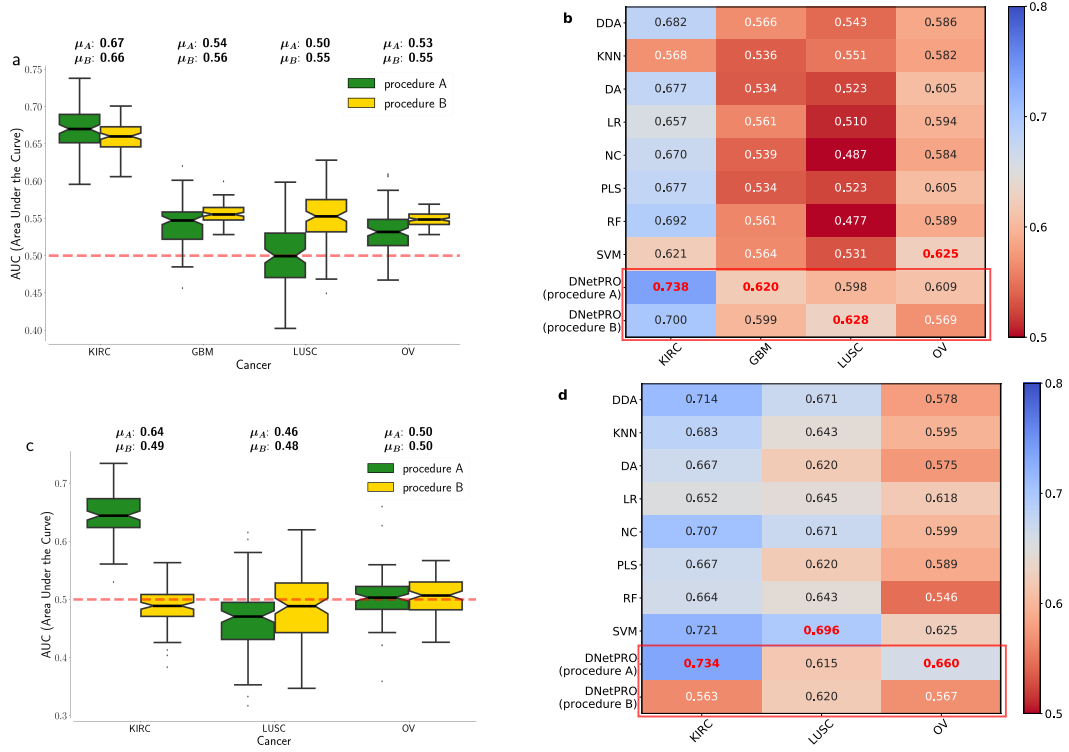


Figure 1.8: Results obtained by the DNetPRO algorithm pipeline on the four Synapse miRNA and RPPA tumors datasets. **(a, c)** Distributions of AUC scores obtained over the four datasets. Green box-plots: results using procedure *A* of DnetPRO; yellow box-plots: results obtained using procedure *B*. **(b, d)** Comparison of DNetPRO with the methods used in [31]. The reported values are the max AUC values obtained over the 10-Fold cross-validation procedure.

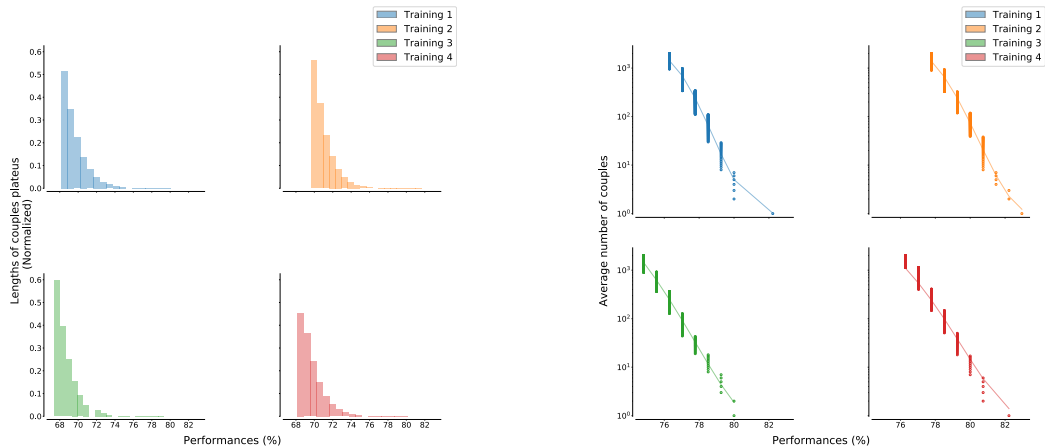


Figure 1.9: Analysis of ranked pairs distributions according to the performance score obtained in the training step. **(a)** The distribution of plateau lengths is approximately exponential. **(b)** Average number of pairs with the same score value: this behavior is typical in ranking order distribution and it can be fitted by the relation  $f(x) = A(M + 1 - r)^b / r^a$  as shown in [21], where  $r$  is the rank value,  $M$  its maximum value,  $A$  a normalization constant and  $(a, b)$  two fitting exponents.

As in other cases of ranked values [21], we can fit these ranking distributions with a combination of power-law functions obtaining a good agreement with experimental points (Fig. 1.9(b)).

We also observed that *star*-networks frequently appear with one variable highly connected to many others which are only connected with it. This happens when a variable has a strong discriminating power, to which other possibly less relevant variables get linked for noisy fluctuations.

As stated before, we suggest that these variables (pendant nodes in the star network) can be removed from the signature without significantly affecting its performance. The procedure can be applied for one single step (in order to remove nodes pending from a star configuration) or it can be applied recursively, until the signature becomes constituted only by the 2-core network (i.e. with all nodes having degree  $\geq 2$ ). Empirical analysis performed on real data has shown that the removal of these variables does not affect significantly the signature performance and in the meanwhile it allows a significant reduction of its dimensionality. Since there is no clear theoretical explanation of this behavior, we suggest to introduce this step only optionally, since it is not easy to quantify the risk of loosing relevant information from the removed variables.

The underlying idea is that the more connected are the nodes, the more the variables in the signature “work well” together, a plausible hypothesis given by the linear sample separation surface provided by the Discriminant classifier. Moreover, the network structure of the signature suggests further considerations about the relevance of a variable as a function of its role in the network (e.g. node centrality such as degree or betweenness centrality).

#### 1.4.5 Characterization of signature overlap

In the analysis of the Synapse dataset we used a complex pipeline of cross-validation (ref Fig. 1.6) to obtain a sufficient statistics. The DNetPRO algorithm was designed to work on a single dataset since the signature extraction can involve different variables for different data subdivisions. In our application, we divide the dataset into a training-test subdivision and the signature were extracted along a 10-fold cross-validation over the training set. This kind of setup could produce 10 totally different signatures, in the worst case. Moreover, we replicated our simulation for 100 repetitions and thus a set of 1000 totally independent signatures were extracted.

Starting from this large subset of variables, we can evaluate the robustness of the DNetPRO algorithm in the variable identifications studying the overlap between these signatures. From a statistical point-of-view it is quite unlikely that the same set of variables were included into all the extracted signatures, especially on this application, in which the variable roles are assumed by genes. On the other hand, the overlap of these signatures could highlight a statistical significance of some variables and thus genes related to the understudied tumors.

As case study, we analyzed only the KIRC mRNA dataset, in which the extracted signatures ranged from 4 to 650 genes ( $\mu = 382$  genes). For each gene we counted its occurrences along the 1000 signatures. The same analysis was performed taking into account the signatures generated using the  $K$ -best score variables (ref. 1.2 for further information) and a random features extraction. In Fig. 1.10 the genes distribution obtained by the three methods are shown.

Both DNetPRO and  $K$ -best feature extraction algorithms identified a core set of genes common to the full set of signatures. The  $K$ -best algorithm appears more stable than the DNetPRO algorithm and it is easier to find the same genes along the extracted signatures. This behavior could be associated to the problems highlighted also in the toy model simulations (ref. 1.2): the DNetPRO algorithm is able to identify only one signature but the

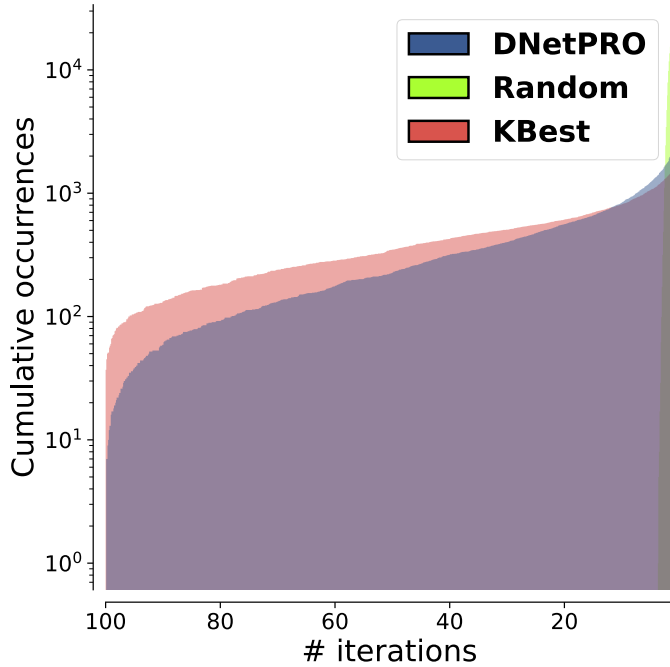


Figure 1.10: Signatures overlap obtained in the KIRC mRNA datasets. Genes occurrences of the 1000 DNetPRO signatures extracted from the Synapse pipeline (blue). Genes occurrences of the 1000  $K$ -best variables extracted from the Synapse pipeline (red): the number of genes ( $K$ ) is the same of the corresponding DNetPRO signature. Genes occurrences of 1000 random signatures (yellow).

informative features (genes) could not co-operate in the same network-signature and thus they could be discarded. The DNetPRO signatures are, in fact, very small compared to the number of variables and thus only small network components were extracted, which are very closed to star-networks. Despite the discrepancy between the signatures we have a core of 18 genes which occurs in at least the 95% of both signatures and 8 of them are in the 99% of both signatures.

The common genes were also mapped on public databases (TISIDB [27] and Oncotarget [?], which link tumors to related genes. We found 14/18 genes as informative probes for the KIRC tumor in the TISIDB and 7 of them were also found in the Oncotarget database<sup>18</sup>. Taking into account the core set of 8 genes, we found 3 of them on Oncotarget database and 7 of them on the TISIDB. The only exception was given by the LOC388796 gene, which was not found in any database.

The random feature extraction method is not even comparable with the others and it simply represents a null model.

## 1.5 Cytokinoma dataset

Increasing evidence suggests that inflammation is involved in Alzheimer’s disease (AD) pathogenesis. Elevated peripheral levels of different cytokines and chemokines in subjects affected by AD compared with healthy control (CTL) have emphasized the role of peripheral inflammation in the disease. Thus, these proteins can represent specific factors of disease development and progression. Considering the cross-talking between the cen-

<sup>18</sup> The list of genes in the TISIDB cover “only” 988 genes. From our list we have only one gene which was found in the Oncotarget database and not in the TISIDB. This gene misses in the TISIDB so we can not evaluate its importance.

tral nervous system and the periphery, the inflammatory analytes may provide utility as biomarkers to identify AD at earlier stages, in particular for the diagnosis of Mild Cognitive Impairment (MCI), a condition at risk of development of dementia. AD is a major neurocognitive disorder and the most common cause of dementia in the old age, accounting for 60% to 80% of all causes. During the past decade, a conceptual shift occurred in the field of AD considering the disease as a continuum. In this context, there is an urgent need for biomarkers identification able to accurately detect AD in an early stage, before the appearance of neurologic signs. An early diagnosis can hopefully lead to a better and more effective treatment, which could potentially limit neuronal damage and prevent the development of overt AD. An emerging field in the study of neuroinflammation is the sex-related differences: in the last years, gender studies have been increasingly developed with the aim to adopt gender differences as a key to interpretation many diseases, including neurodegenerative diseases.

Experimental data showed that many mechanisms are involved in AD pathogenesis including neuroinflammation. The dysregulation of cytokines and chemokines is a central feature in the development of neuroinflammation, neurodegeneration, and demyelination both in the central and peripheral nervous systems. Among many chemokines and cytokines, pro-inflammatory IFN $\alpha$ 2, TNF $\alpha$ , and IL-1 $\alpha$  are described as heterogeneously implicated in AD pathogenesis.

The interactive network of cytokines/chemokines, defined as “cytokinome”, is extremely complex. Using the DNetPRO algorithm as statistical feature selection method, we might discriminate the groups and propose a useful tool to follow the progression and evolution of AD from its early stages, also in light of gender differences. With this study, we aimed first at the identification of a potential proteins profile able to discriminate AD, MCI and CTL and, therefore identify a potential early and easy to get a diagnostic marker of subjects at risk.

Further information about this work can be found in the original paper [5].

### 1.5.1 Dataset

In this case-control observational study, we evaluated 289 old-age subjects referred to our Geriatric Memory Clinic. The dataset comprises 189 female and 100 male individuals with a mean age of 78.6 ( $\pm 7.5$ ) years. The date were provided by the co-authors of this project at the Institute of Gerontology and Geriatrics at the University of Perugia (Department of Medicine). For each patient a set of 26 cytokine expression level were computed with the additional information about subject set, age and diagnosis label (AD, MCI or CTL). Of the 289 enrolled subjects, the whole set of cytokines was available for 284 subjects (98%), specifically 87/88 CTL (99%), 70/73 MCI (96%), 127/129 AD (98%).

To approximate normal distribution, plasma cytokines and chemokines were log-transformed for data analyses. For the analysis of single cytokines with respect to the CTL, MCI and AD group, we designed a linear model analysis, with the value of each cytokine as a linear combination of the subject group (with CTL samples as the baseline, and MCI, AD as conditions), age and sex, as factors (the formula representation would be “cytokine  $\sim$  group + sex + age”). The last two were included as possible confounding factors, even if the analyses revealed that their role for each cytokine is marginal. Only IFN $\alpha$ 2, IL-1 $\alpha$ , and MCP-1 differed among groups after correction for age and sex. A threshold  $p < 0.05$  was considered for significance at all levels (group, sex or age).

Then we applied the DNetPRO algorithm looking for a signature capable of discriminating between CTL and AD: to this purpose, we performed a Hold-Out cross-validation procedure to identify the cytokine signature, considering 2/3 of samples to train the model and then we tested the signature performance on the remaining 1/3 of the total samples. In this analysis we did not separate male from female samples, to avoid the bias given

by the uneven number of samples in these two groups, and since previous analysis at a single-cytokine level did not find significant differences due to sex. Then, we classified MCI samples with the CTL-AD signature obtained in the previous step, that allowed labeling MCI samples as CTL or non-CTL.

### 1.5.2 Results

The best signature identified to discriminate between CTL and AD subjects is composed of three cytokines, IFN $\alpha$ 2, TNF $\alpha$ , and IL-1 $\alpha$ . Its total accuracy on the CTL-AD test set is 65.27% (with 61% CTL and 66% AD correctly classified). The sensitivity/specificity values for classification is reported in Tab. 1.2.

	<b>Accuracy</b>	<b>Sensitivity</b>	<b>Specificity</b>	<b>Prediction</b>	<b>Sensitivity</b>	<b>Specificity</b>
	AD vs. CTL	AD	CTL	MCI as non-CTL	MCI	CTL
Men	16/25 (64.00%)	8/12 (66.67%)	8/13 (61.54%)	15/26 (57.69%)	15/26 (57.69%)	24/36 (66.67%)
Women	33/48 (68.75%)	27/38 (71.05%)	6/10 (60.00%)	41/47 (87.23%)	41/47 (87.23%)	23/51 (45.09%)
Total	47/72 (65.24%)	36/54 (66.66%)	11/18 (61.11%)	62/73 (84.93%)	62/73 (84.93%)	36/87 (41.38%)

Table 1.2: The sensitivity/specificity values for AD vs CTL classification by the 3-protein signature, for the total sample dataset and stratified by sex. The second table shows the result of predictions of MCI samples with the same signature as non-CTL samples. In this case the sensitivity and specificity were computed in relation to the CTL in the training set.

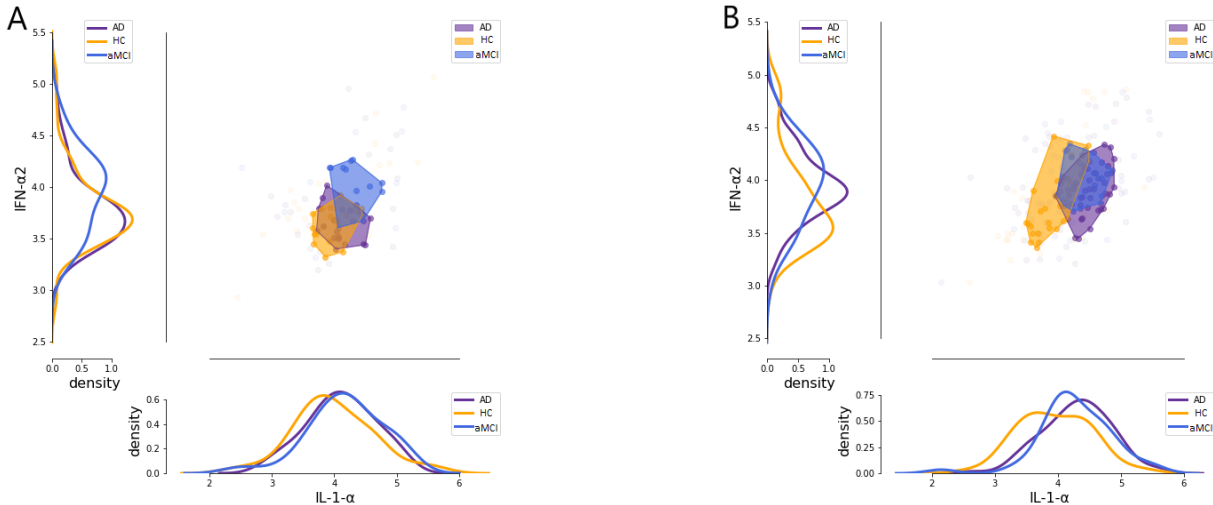


Figure 1.11: **(A)** Scatter plot of IL-1 $\alpha$  and IFN- $\alpha$ , and distribution plot for the single cytokines along the axes, stratified by diagnostic group (AD, CTL, and MCI) in **males**. In this case, the HC group is less separated from MCI and AD. **(B)** Scatter plot of IL-1 $\alpha$  and IFN- $\alpha$ , and distribution plot for the single cytokines along the axes, stratified by diagnostic group (AD, CTL, and MCI) in **females**. In this case, the HC group is well separated from MCI and AD.

Applying this signature to classify MCI vs CTL samples, it correctly predicted 84.93% of MCI as “non-CTL”. Two cytokines from the signature, IFN $\alpha$ 2 and IL-1 $\alpha$ , showed a significant difference between groups also at a single cytokine level in previous analyses.

We plotted them as a representative in all population and stratified the scatter plots by sex (ref Fig. 1.11 A, B). The CTL group resulted better separated from MCI and AD in women as compared with men. The trajectory of the subject groups moves from CLT to AD, and interestingly the identified signature is able to differentiate MCI from CLT better than from AD. This is a promising result since it seems more useful to recognize MCI from CLT than full-blown AD from CLT. Probably the poor sensibility in detecting AD could be linked to the disease evolution that makes nebulous and vague the cytokine pattern in the brain of these patients, as confirmed from several studies that found both up-regulation and down-regulation of many cytokines in AD cerebral samples. This fact could be more accentuated in our population of old age subjects in which markers of aging are often mixed with those of dementia.

In this study we show that: 1) an easy to get cytokines signature composed of three molecules - IFN $\alpha$ 2, TNF $\alpha$ , and IL-1 $\alpha$  - is able to discriminate the studied groups; 2) the combination of IFN $\alpha$ 2 and IL-1 $\alpha$  able to distinguish CTL from MCI and AD better in women than in men. Sex (referred to biological differences) and gender (psychosocial and cultural differences) affect human brain biology throughout individual lifespans, affecting male and female cognitive functions differently. Epidemiological studies show that women have a higher risk of AD as well as a higher dementia prevalence, particularly in the old age, as compared with men.

In conclusion, the identified cytokinome signature shows a good accuracy in differentiating MCI from CTL, especially in female. Understanding sex differences will help to define individualized preventive and treatment interventions for AD.

## 1.6 Bovine Dataset

Paratuberculosis or Johne's disease (JD) in cattle is a chronic granulomatous gastroenteritis caused by infection with *Mycobacterium avium subspecies paratuberculosis* (MAP). JD is not treatable; therefore the early identification and isolation of infected animals is a key point to reduce its incidence worldwide. In this work DNetPRO algorithm was applied to RNAseq experimental data of 5 cattle positive to MAP infection compared to 5 negative uninfected controls. The purpose was to find a small set of differentially expressed genes able to discriminate between infected animals in a pre-clinical phase. Results of the DNetPRO algorithm identified a small set of 10 transcripts that differentiate between potentially infected, but clinically healthy, animals belonging to paratuberculosis positive herds and negative unexposed animals. Furthermore, the same set of 10 transcripts differentiate negative unexposed animals from positive animals based on the results of the ELISA test<sup>19</sup> for bovine paratuberculosis and fecal culture. Within the 10 transcripts that together had good discriminative potential, 5 (TRPV4, RIC8B, IL5RA, ERF and CDC40) show significant differential expression between the three groups while the remaining 5 transcripts (RDM1, EPHX1, STAU1, TLE1, ASB8) did not show a significant differences in at least one of the pairwise comparisons. In conclusion, the discriminant analysis described here identified a set of 10 genes that discriminate between the exposed and sero-converted animals. When tested in a larger cohort, these finding lead the possible use of RNA expression analysis as new diagnostic test for paratuberculosis. Such a signature could allow early interventions to reduce the sanitary and economic burden, and to reduce the risk of infection spreading.

In the next sections a description of the dataset and of main DNetPRO results will be discussed. Further information can be found in the original paper [20].

---

<sup>19</sup> The enzyme-linked immunosorbent assay. It is a common diagnostic tool as well as a quality control check in various bio-medical industries and in medicine.

### 1.6.1 Dataset

Paratuberculosis or Johne’s disease (JD) in cattle is a chronic granulomatous gastroenteritis caused by infection with *Mycobacterium avium subspecies paratuberculosis* (MAP). JD is present worldwide, is a welfare issue and causes significant economic losses. Cattle are usually infected as young calves but typically do not show clinical signs before 24 months of age, however not all infected animals progress to clinical disease. JD is not treatable, therefore the early identification and isolation of infected animals, before they start shedding the bacteria, is a key point to reduce its incidence in cattle herds worldwide. In addition, an association between MAP and Crohn’s disease (CD) in humans has been suggested and intensively explored. Given the economic losses and welfare concerns for livestock, and possible human health risk, the research interest in JD has been driven by the substantial difficulty in early diagnosis of infected animals and the exploration of potentially new diagnostic techniques.

The dataset used in this work was previously discussed and generated by some of the authors of the original paper. In detail, the dataset used comprised 15036 transcripts from 15 samples, classified as “serologically negative non exposed cows/healthy” (5 samples, labeled as NN), “serologically negative exposed cows/ infected” (5 samples, NP) and “serologically positive cows/clinical” (5 samples, PP). Only transcripts with non-zero measures for all samples were considered, reducing the dataset to 13529 transcripts.

All data generated or analyzed during this study is available upon request, furthermore all transcript counts per sample are given as supplementary information files of the original paper.

### 1.6.2 Bovine Signature

In the context of high-throughput data analysis, a challenge is the search for an optimal choice of variables (a “signature”) to classify groups of samples or regress trends with optimal performance and minimum dimensionality. Usually high-throughput omics data (e.g. transcriptomics, ge-nomics, methylomics) provide datasets with few tens to hundreds of samples, and often 1000 times larger numbers of variables. The objective of dimensionality reduction through the choice of an optimal signature is twofold: 1) the identification of relevant variables, that should separate the signal from the noise (i.e. variables not significantly associated to, or descriptive of the studied process); 2) in a practical context, it is important to establish future diagnostic criteria that can be implemented in cheap and simple toolkits, such as PCR cards or dedicated microarray chips, that usually test a small number of transcripts (ranging from tens to hundreds, at most). The quantity of samples compared to the available features of this work, join with the final purposes of this kind of analysis, set the well-known ill-posed problem conditions for which the DNetPRO algorithm was thought.

Since the number of sample is drastically small no robust cross-validation procedure can be applied. So we focused on the identification of a putative gene-signature able to discriminate between NN and NP samples, leaving the PP data as validation set. In this case we hypothesize that PP samples will be classified more closely with NP sample rather than NN as exposed, possibly infected samples, should be more similar to positive samples, than to negative controls.

Starting from the top-performing couples of transcripts, we obtained an initial signature of 123 different transcripts (Fig 1.12(a), all the nodes), capable to correctly classify 4 out of the 5 NN samples (80%) and all 5 NP samples (100% performance). The average performance was therefore 90% with Matthews correlation coefficient  $MCC = 0.82$ . Processing the 123-transcript network by removing all pendant nodes (i.e. removing all

---

<sup>21</sup> The figure was generated using a custom network visualizer described in Appendix C - BlendNet.

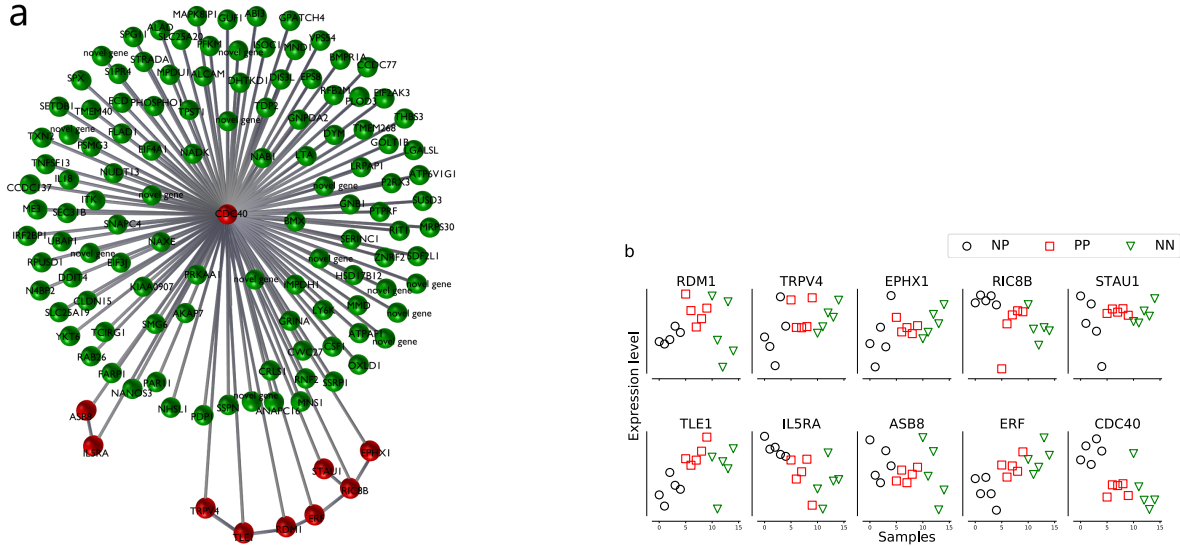


Figure 1.12: (a) Plot of the 123-transcript network, with a details of the 10-probe signature (red nodes)<sup>21</sup>. (b) Transcript levels for the 10 genes belonging to the classification signature identified by the combinatorial discriminant analysis (CDA). Some transcripts (EPHX1, RIC8B, IL5RA, ERF, CDC40) show a clear trend between 5 animals serologically positive to the ELISA test for MAP (PP), 5 exposed serologically negative (NP) and 5 serologically negative unexposed control animals (NN).

single transcripts belonging to only one best-performing couple) we obtained a final signature with 10 transcripts with a 100% performance classifying all NN and NP samples (Fig 1.12(a), only red nodes). As it can be seen, many nodes are directly connected to the central node (belonging to the 10-transcript signature), while only the 10 transcripts of the signature are also connected between each other.

Principal Component Analysis of the 10-transcript signature showed that in many cases there was a progressive increase or decrease in the transcript levels when passing from a healthy (NN) sample to a positive (PP) sample, passing through the infected (NP) sample class. Fig 1.12(b) shows the expression levels of the transcripts belonging to the signature for all samples.

To further validate the goodness of the signature, we generated 10000 different signatures with 10 randomly chosen transcripts, and then applied a Leave-One-Out cross validation procedure to classify all 15 samples with these signatures. Comparing the performance of the random signatures with the true 10-transcript signature, only 50 of these signatures (corresponding to 0.5% of the random signature distribution) produced better performance than our signature in terms of classification performance, confirming its high significance.

We even characterized the possible biological role of the signature genes, among the significantly differentially expressed genes, the cell division cycle 40 gene (CDC40) showed the smallest fold change between classes. However in the identified signature the CDC40 gene is the most central node associated with the health status of the animals related to JD. CDC40 was also under expressed in the NP and PP groups, compared with the NN group and it has been shown to be involved in clathrin mediated endocytosis from a biological point-of-view. Clathrin is the best characterized coat protein involved in the endocytosis process, specifically in receptor-mediated-internalization. *Mycobacterium paratuberculosis* enters the host macrophages, its primary target cell, and manages to survive within their phagosome. It is possible that the under-expression of CDC40 in infected and sick animals compared to unexposed animals may be associate with down regulation of macrophage

genes post mycobacterial invasion, facilitating the survival of the pathogen with the host target cell.

Interestingly within the set of 10 discriminating transcripts, in addition to CDC40, others show links with immune response mechanisms, these include IL5RA, ERF and TRPV4. These genes potentially have functions related to the biology of progression of JD. Also for the other genes of the final 10-transcript signature a possible biological interpretation related to JD was given (see the original paper for further descriptions).

In conclusion, the DNetPRO algorithm identified a set of 10 genes, the expression levels of which could discriminate between the exposed and sero-converted animals. These finding lead the possible use of RNA expression analysis as new diagnostic test for JD. In particular the approach may be able to identify infected animals prior to sero-conversion, prior to a positive ELISA test result. However, further tests for specificity and validation in a larger cohort are required.

# Bibliography

- [1] A. Battle, S. Mostafavi, X. Zhu, J. B. Potash, M. M. Weissman, C. McCormick, C. D. Haudenschild, K. B. Beckman, J. Shi, R. Mei, A. E. Urban, S. B. Montgomery, D. F. Levinson, and D. Koller. Characterizing the genetic basis of transcriptome diversity through rna-sequencing of 922 individuals. *Genome Research*, 2014.
- [2] J. S. Beckmann and D. A. Lew. Reconciling evidence-based medicine and precision medicine in the era of big data: challenges and opportunities. In *Genome Medicine*, 2016.
- [3] S. Behnel, R. Bradshaw, C. Citro, L. Dalcin, D. Seljebotn, and K. Smith. Cython: The best of both worlds. *Computing in Science Engineering*, 13(2):31–39, 2011.
- [4] R. Bellman and K. M. R. Collection. *Adaptive Control Processes: A Guided Tour*. Princeton Legacy Library. Princeton University Press, 1961.
- [5] V. Boccardi, L. Paolacci, D. Remondini, E. Giampieri, G. Poli, N. Curti, R. Cecchetti, A. Villa, C. Ruggiero, S. Brancorsini, and P. Mecocci. Cognitive decline and alzheimer’s disease in the old age: identified a sex specific “cytokinome signature”. 2019.
- [6] C. Cenik, E. S. Cenik, G. W. Byeon, F. Grubert, S. I. Candille, D. Spacek, B. Al-sallakh, H. Tilgner, C. L. Araya, H. Tang, E. Ricci, and M. P. Snyder. Integrative analysis of rna, translation, and protein levels reveals distinct regulatory variation across humans. *Genome Research*, 2015.
- [7] I. S. Chan and G. S. Ginsburg. Personalized medicine: Progress and promise. *Annual Review of Genomics and Human Genetics*, 12(1):217–244, 2011. PMID: 21721939.
- [8] N. Curti. DNetPRO pipeline: Implementation of the dnetpro pipeline for tcga datasets. <https://github.com/Nico-Curti/DNetPRO>, 2019.
- [9] N. Curti, E. Giampieri, G. Levi, G. Castellani, and D. Remondini. Dnetpro: A network approach for low-dimensional signatures from high-throughput data. *bioRxiv*, 2019.
- [10] N. Curti, E. Giampieri, C. Mizzi, A. Fabbri, A. Bazzani, G. Castellani, and D. Remondini. A network approach for dimensionality reduction from high-throughput data. volume proceedings, 2019.
- [11] L. Dagum and R. Menon. Openmp: an industry standard api for shared-memory programming. *Computational Science & Engineering, IEEE*, 5(1):46–55, 1998.
- [12] L. Eckhard. A universal selection method in linear regression models. *Open Journal of Statistics*, 2, 2012.
- [13] C. Greene, J. Tan, M. Ung, J. Moore, and C. Cheng. Big data bioinformatics. *Journal of cellular physiology*, 229(12), 2014.

- [14] I. Guyon, J. Weston, S. Barnhill, and V. Vapnik. Gene selection for cancer classification using support vector machines. *Mach. Learn.*, 2002.
- [15] R. R. Hocking. A biometrics invited paper. the analysis and selection of variables in linear regression. *Biometrics*, 32(1):1–49, 1976.
- [16] J. J. Hughey and A. J. Butte. Robust meta-analysis of gene expression using the elastic net. *Nucleic Acids Research*, 2015.
- [17] T. M. Johnson. Perspective on precision medicine in oncology. *Pharmacotherapy: The Journal of Human Pharmacology and Drug Therapy*, 37(9):988–989, 2017.
- [18] J. Koster and S. Rahmann. Snakemake - a scalable bioinformatics workflow engine. *Bioinformatics*, 28:2520–2522, 08 2012.
- [19] D. Kumari and R. Kumar. Impact of biological big data in bioinformatics. *International Journal of Computer Applications*, 101(11):22–24, 2014.
- [20] M. Malvisi, N. Curti, D. Remondini, G. Gandini, F. Palazzo, G. Pagnacco, J. L. Williams, and G. Minozzi. Combinatorial discriminant analysis applied to rnaseq data reveals a set of 10 transcripts as signatures of infection of cattle with mycobacterium avium subsp. paratuberculosis. 2019.
- [21] G. Martínez-Mekler, R. A. Martínez, M. B. del Río, R. Mansilla, P. Miramontes, and G. Cocho. Universality of rank-ordering distributions in the arts and sciences. *PLoS One*, 11 2009.
- [22] V. Marx. The big challenges of big data. *Nature Reviews*, 498(255), 2013.
- [23] M. McKinney. Human genome project information. *Reference Reviews*, 26(3):38–39, 2012.
- [24] C. Mizzi, A. Fabbri, S. Rambaldi, F. Bertini, N. Curti, S. Sinigardi, R. Luzi, G. Venturi, M. Davide, G. Muratore, A. Vannelli, and A. Bazzani. Unraveling pedestrian mobility on a road network using icts data during great tourist events. *EPJ Data Science*, 7(1):44, Oct 2018.
- [25] H. Pang, S. L. George, K. Hui, and T. Tong. Gene selection using iterative feature elimination random forests for survival outcomes. *IEEE/ACM Transactions on Computational Biology and Bioinformatics / IEEE*, 2012.
- [26] J. A. Reuter, D. V. Spacek, and M. P. Snyder. High-throughput sequencing technologies. *Molecular Cell*, 2015.
- [27] B. Ru, C. N. Wong, Y. Tong, J. Y. Zhong, S. S. W. Zhong, W. C. Wu, K. C. Chu, C. Y. Wong, C. Y. Lau, I. Chen, N. W. Chan, and J. Zhang. TISIDB: an integrated repository portal for tumor-immune system interactions. *Bioinformatics*, 03 2019. btz210.
- [28] K. Scotlandi, D. Remondini, G. Castellani, M. C. Manara, F. Nardi, L. Cantiani, M. Francesconi, M. Mercuri, A. M. Caccuri, M. Serra, S. Knuutila, and P. Picci. Overcoming resistance to conventional drugs in ewing sarcoma and identification of molecular predictors of outcome. *Journal of Clinical Oncology*, 27(13):2209–2216, 2009. PMID: 19307502.
- [29] J. Siek, L.-Q. Lee, and A. Lumsdaine. Boost graph library. <http://www.boost.org/libs/graph/>, June 2000.

- [30] C. Terragna, D. Remondini, M. Martello, E. Zamagni, L. Pantani, F. Patriarca, A. Pezzi, G. Levi, M. Offidani, I. Proserpio, G. De Sabbata, P. Tacchetti, C. Can-gialosi, F. Ciambelli, C. V. Viganò, F. A. Dico, B. Santacroce, E. Borsi, A. Brioli, G. Marzocchi, G. Castellani, G. Martinelli, A. Palumbo, and M. Cavo. The genetic and genomic background of multiple myeloma patients achieving complete response after induction therapy with bortezomib, thalidomide and dexamethasone. *Oncotarget*, 2016.
- [31] Y. Yuan, E. M. Van Allen, L. Omberg, N. Wagle, A. Amin-Mansour, A. Sokolov, L. A. Byers, Y. Xu, K. R. Hess, L. Diao, L. Han, X. Huang, M. S. Lawrence, J. N. Weinstein, J. M. Stuart, G. B. Mills, L. A. Garraway, A. A. Margolin, G. Getz, and H. Liang. Assessing the clinical utility of cancer genomic and proteomic data across tumor types. *Nature Biotechnology*, 32(7):644–652, 2014.